CLEO-CONF 05-02
LP2005-440

Observation of $\psi(3770) \to \pi\pi J/\psi$ and Measurement of $\Gamma_{ee}(\psi(2S))^*$

T. K. Pedlar,[1] D. Cronin-Hennessy,[2] K. Y. Gao,[2] D. T. Gong,[2] J. Hietala,[2] Y. Kubota,[2] T. Klein,[2] B. W. Lang,[2] S. Z. Li,[2] R. Poling,[2] A. W. Scott,[2] A. Smith,[2] S. Dobbs,[3] Z. Metreveli,[3] K. K. Seth,[3] A. Tomaradze,[3] P. Zweber,[3] J. Ernst,[4] H. Severini,[5] D. M. Asner,[6] S. A. Dytman,[6] W. Love,[6] S. Mehrabyan,[6] J. A. Mueller,[6] V. Savinov,[6] Z. Li,[7] A. Lopez,[7] H. Mendez,[7] J. Ramirez,[7] G. S. Huang,[8] D. H. Miller,[8] V. Pavlunin,[8] B. Sanghi,[8] I. P. J. Shipsey,[8] G. S. Adams,[9] M. Cravey,[9] J. P. Cummings,[9] I. Danko,[9] J. Napolitano,[9] Q. He,[10] H. Muramatsu,[10] C. S. Park,[10] E. H. Thorndike,[10] T. E. Coan,[11] Y. S. Gao,[11] F. Liu,[11] M. Artuso,[12] C. Boulahouache,[12] S. Blusk,[12] J. Butt,[12] O. Dorjkhaidav,[12] J. Li,[12] N. Menaa,[12] R. Mountain,[12] R. Nandakumar,[12] K. Randrianarivony,[12] R. Redjimi,[12] R. Sia,[12] T. Skwarnicki,[12] S. Stone,[12] J. C. Wang,[12] K. Zhang,[12] S. E. Csorna,[13] G. Bonvicini,[14] D. Cinabro,[14] M. Dubrovin,[14] R. A. Briere,[15] G. P. Chen,[15] J. Chen,[15] T. Ferguson,[15] G. Tatishvili,[15] H. Vogel,[15] M. E. Watkins,[15] J. L. Rosner,[16] N. E. Adam,[17] J. P. Alexander,[17] K. Berkelman,[17] D. G. Cassel,[17] V. Crede,[17] J. E. Duboscq,[17] K. M. Ecklund,[17] R. Ehrlich,[17] L. Fields,[17] R. S. Galik,[17] L. Gibbons,[17] B. Gittelman,[17] R. Gray,[17] S. W. Gray,[17] D. L. Hartill,[17] B. K. Heltsley,[17] D. Hertz,[17] C. D. Jones,[17] J. Kandaswamy,[17] D. L. Kreinick,[17] V. E. Kuznetsov,[17] H. Mahlke-Krüger,[17] T. O. Meyer,[17] P. U. E. Onyisi,[17] J. R. Patterson,[17] D. Peterson,[17] E. A. Phillips,[17] J. Pivarski,[17] D. Riley,[17] A. Ryd,[17] A. J. Sadoff,[17] H. Schwarthoff,[17] X. Shi,[17] M. R. Shepherd,[17] S. Stroiney,[17] W. M. Sun,[17] D. Urner,[17] T. Wilksen,[17] K. M. Weaver,[17] M. Weinberger,[17] S. B. Athar,[18] P. Avery,[18] L. Breva-Newell,[18] R. Patel,[18] V. Potlia,[18] H. Stoeck,[18] J. Yelton,[18] P. Rubin,[19] C. Cawlfield,[20] B. I. Eisenstein,[20] G. D. Gollin,[20] I. Karliner,[20] D. Kim,[20] N. Lowrey,[20] P. Naik,[20] C. Sedlack,[20] M. Selen,[20] E. J. White,[20] J. Williams,[20] J. Wiss,[20] K. W. Edwards,[21] and D. Besson[22]

(CLEO Collaboration)

[1]*Luther College, Decorah, Iowa 52101*
[2]*University of Minnesota, Minneapolis, Minnesota 55455*
[3]*Northwestern University, Evanston, Illinois 60208*
[4]*State University of New York at Albany, Albany, New York 12222*
[5]*University of Oklahoma, Norman, Oklahoma 73019*
[6]*University of Pittsburgh, Pittsburgh, Pennsylvania 15260*
[7]*University of Puerto Rico, Mayaguez, Puerto Rico 00681*
[8]*Purdue University, West Lafayette, Indiana 47907*
[9]*Rensselaer Polytechnic Institute, Troy, New York 12180*
[10]*University of Rochester, Rochester, New York 14627*
[11]*Southern Methodist University, Dallas, Texas 75275*
[12]*Syracuse University, Syracuse, New York 13244*
[13]*Vanderbilt University, Nashville, Tennessee 37235*
[14]*Wayne State University, Detroit, Michigan 48202*
[15]*Carnegie Mellon University, Pittsburgh, Pennsylvania 15213*
[16]*Enrico Fermi Institute, University of Chicago, Chicago, Illinois 60637*
[17]*Cornell University, Ithaca, New York 14853*

[18] *University of Florida, Gainesville, Florida 32611*
[19] *George Mason University, Fairfax, Virginia 22030*
[20] *University of Illinois, Urbana-Champaign, Illinois 61801*
[21] *Carleton University, Ottawa, Ontario, Canada K1S 5B6*
and the Institute of Particle Physics, Canada
[22] *University of Kansas, Lawrence, Kansas 66045*

Abstract

Using $e^+e^- \to XJ/\psi$, $J/\psi \to \ell^+\ell^-$ events taken at $\sqrt{s}$=3773 MeV with the CLEO detector operating at CESR, we observe signals for the direct decays $\psi(3770) \to XJ/\psi$, $X = \pi^+\pi^-$ (13σ significance) and $\pi^0\pi^0$ (3.8σ significance). We determine the cross sections and branching fractions for these modes, $\mathcal{B}(\psi(3770) \to \pi^+\pi^- J/\psi) = (189 \pm 22^{+7}_{-4}) \times 10^{-5}$ and $\mathcal{B}(\psi(3770) \to \pi^0\pi^0 J/\psi) = (87 \pm 33 \pm^{+4}_{-3}) \times 10^{-5}$, where listed errors are statistical and systematic, respectively. The signals for decays with $X = \eta$ and π^0 are statistically inconclusive. The XJ/ψ event sample has a large contribution from the radiative return process $e^+e^- \to \gamma\psi(2S) \to \gamma XJ/\psi$ and is used to measure $\Gamma_{ee}(\psi(2S)) = 2145 \pm 85$ eV (statistical and systematic errors combined), consistent with and more precise than individual or combined previous measurements. All results are preliminary.

*Submitted to the XXII International Symposium on Lepton and Photon Interactions at High Energies, June 30-July 5, 2005, Uppsala, Sweden

I. INTRODUCTION

The $\psi(3770)$ charmonium state decays most copiously into $D\bar{D}$ pairs. As each of the $\psi(3770)$ and $\psi(2S)$ mass eigenstates is expected to be a mixture of the 1^3D_1 and 2^3S_1 angular momentum eigenstates, other $\psi(2S)$-like decays for $\psi(3770)$ are expected [1–7]. Decays to light hadrons are explored in two other submissions [8, 9] to this Conference and those involving radiative transitions through χ_{cJ} elsewhere [10]. Because more than half of $\psi(2S)$ decays contain a J/ψ in the final state, the $2\,^3S_1$ admixture in $\psi(3770)$ implies that similar transitions occur from this state as well. Transitions of this sort from the $1\,^3D_1$ eigenstate can also occur. Theoretical estimates [3–6] for the rate of this latter process, based on a QCD multipole expansion, are very uncertain, allowing for branching fractions at the few tenths percent level. BES reported the first sighting of a $\psi(3770)$ non-$D\bar{D}$ decay [11], at 3σ significance, with $\mathcal{B}(\psi(3770) \to \pi^+\pi^- J/\psi) = (0.34 \pm 0.14 \pm 0.09)\%$.

The width for $\psi(3770) \to \pi^+\pi^- J/\psi$ can be brought to bear on the interpretation [12, 13] of the $X(3872)$ [14]: a width the size that BES [11] measured, or larger, enhances the possibility that $X(3872)$ is a conventional $1\,^3D_2$ charmonium state. A significantly smaller value would favor other quantum number assignments (the weakly bound DD^* molecule hypothesis, or a hybrid), which recent developments [15–17] seem to favor.

Voloshin [18] posits that the $c\bar{c}$ purity of the $\psi(2S)$ and $\psi(3770)$ and the nature of their mixing can be probed by measuring the rates for $\psi(3770) \to \pi^0 J/\psi$ and $\psi(3770) \to \eta J/\psi$. Large rates for these modes could indicate a 4-quark component in these two charmonium states that would also explain other features of their decays.

In this paper we describe a search for the XJ/ψ final states, $X = \pi^+\pi^-$, $\pi^0\pi^0$, η, and π^0, in e^+e^- collision data taken at a center-of-mass energy $\sqrt{s}$=3.773 GeV. The data were acquired with the CLEO detector operating at the Cornell Electron Storage Ring (CESR) [19], and correspond to an integrated luminosity of 281 pb^{-1}. The radiative return process $e^+e^- \to \gamma\psi(2S) \to \gamma XJ/\psi$ must be quantitatively understood in order to validate any signal for $\psi(3770) \to XJ/\psi$. We evaluate what fractions of the observed XJ/ψ events are attributable to $\psi(3770)$ and $\gamma\psi(2S)$ decays. The sample of $\gamma\psi(2S)$ events is also used to measure $\Gamma_{ee}(\psi(2S))$.

The CLEO-c detector [20] features a solid angle coverage of 93% for charged and neutral particles. For the data presented here, the charged particle tracking system operates in a 1.0 T magnetic field along the beam axis and achieves a momentum resolution of $\sim$0.6% at $p = 1$ GeV/c. The cesium iodide (CsI) calorimeter attains photon energy resolutions of 2.2% at $E_\gamma = 1$ GeV and 5% at 100 MeV. The integrated luminosity ($\mathcal{L}$) of the datasets was measured with a relative accuracy of 1.0% using e^+e^-, $\gamma\gamma$, and $\mu^+\mu^-$ events [21]; event counts were normalized with a Monte Carlo (MC) simulation based on the Babayaga [22] event generator.

II. ANALYSIS OVERVIEW

We select fully reconstructed XJ/ψ, $J/\psi \to \ell^+\ell^-$ candidates for each mode with as loose a set of criteria as backgrounds will permit (thereby attempting to minimize systematic effects), determine efficiencies from fully simulated Monte Carlo samples, subtract backgrounds, and normalize to luminosity and the $D\bar{D}$ cross section.

The primary background for $\psi(3770) \to \pi\pi J/\psi$ is the tail of the $\psi(2S)$ resonance and radiative returns to it. By the term "tail of the $\psi(2S)$" we mean the process $e^+e^- \to \gamma\psi(2S)$

in which the photon usually, but not always, goes in the forward direction down the beam pipe. Because there is a long tail to the $\psi(2S)$ Breit-Wigner resonance shape, the radiative photon can take on a range of energies, with a peak near $E_\gamma \sim (3773 - 3686) = 87$ MeV and including arbitrarily close to zero. It is straightforward to estimate the full differential cross section for this tail (see below). The distribution in radiative photon energy for a single fixed beam energy with no spread is shown in Fig. 1. Direct decays from the $\psi(3770)$ and the tail of the $\psi(2S)$ add incoherently [5], so that the $\psi(2S)$ background can be simply subtracted.

In order to prove that we understand the tail, we measure both the "signal" for $\psi(3770) \to XJ/\psi$ as well as the "background" tail of the $\psi(2S)$. The integral of all $\psi(2S)$ radiative return events for a particular X is proportional to $\mathcal{B}(\psi(2S) \to XJ/\psi) \times \Gamma_{ee}(\psi(2S))$, facilitating a precision measurement of $\Gamma_{ee}(\psi(2S))$ by using previously measured CLEO $\psi(2S)$ and $J/\psi \to \ell^+\ell^-$ branching fractions [23, 24]. The Γ_{ee} values thus obtained will be seen to be consistent with (and more precise than) PDG [25] values, showing that we both understand the background and can improve upon knowledge of Γ_{ee}.

III. EVENT SELECTION

We proceed from the starting point of our $\psi(2S) \to XJ/\psi$ analysis [24], but make some adjustments in the selection criteria more appropriate to the situation here.

To select event samples of $J/\psi \to \ell^+\ell^-$, we demand that candidate events fulfill the following requirements: The lepton pair consists of the two highest-momentum tracks in the event which individually satisfy $|\cos\theta| < 0.83$ or $0.85 < |\cos\theta| < 0.93$ (avoiding the barrel-endcap calorimeter overlap region, where lepton identification would be problematic). The lepton candidates must also obey the very loose identification criteria of $E/p > 0.85$ for one electron and $E/p > 0.5$ for the other, or $E/p < 0.25$ and $E/p < 0.5$ in case of muons, where E is the measured calorimetric energy deposition of each track and p is its measured momentum. The invariant mass of the track pair must be consistent with that of a J/ψ, with $m(\ell^+\ell^-) = 3.05 - 3.14\,\mathrm{GeV}$. In order to salvage lepton pairs that have radiated photons and would hence fail the J/ψ mass cut, we add bremsstrahlung photon candidates found within a cone of 100 mrad to the track three-vector at the e^+e^- interaction point. We impose loose restrictions on the absolute momentum and energy of the event: $(E_{J/\psi} + E_{\pi^+\pi^-})/\sqrt{s} = 0.95 - 1.05$, $||p_{J/\psi}| - |p_{\pi^+\pi^-}||/\sqrt{s} < 0.07$.

The accompanying particle(s) X are selected as follows. The $X = \pi^+\pi^-$ and $X = \eta \to \pi^+\pi^-\pi^0$ state is selected from events with at least four charged tracks, and the third and fourth most energetic tracks are taken if they have opposite charge. The first π^0 candidate is taken as the most energetic candidate that has photons which are unmatched to a track, are more than 30 cm from the nearest shower matched to a track, and are not tagged as bremsstrahlung, and have $M(\gamma\gamma)$=80-180 MeV. Candidates for $X = \pi^0\pi^0$ take the first π^0 as above, and the second π^0 as the next most energetic π^0 that contains photons satisfying the same criteria as the first π^0 but does not involve either of the showers in the first π^0 candidate. Candidates for $\eta \to \gamma\gamma$ are defined in an identical manner as π^0's except for the initial mass cut, $M(\gamma\gamma)$=450-650 MeV. Candidates for $\eta \to \pi^+\pi^-\pi^0$ need to fulfill the track and π^0 selection as above and are required to satisfy $M(\pi^+\pi^-\pi^0)$=450-650 MeV.

Final cuts are specific to each final state.

- For $X = \pi^+\pi^-$, the $\pi^+\pi^-$ invariant mass is required to exceed 450 MeV to suppress

radiative Bhabha and muon pair events in which the photon converts and the conversion e^+e^- pair is mistaken for the pion pair. The dipion invariant mass cut is placed at 350 MeV for $\pi^0\pi^0 J/\psi$ events.

- Candidate π^0 and η mesons must satisfy respective mass cuts of 110-150 MeV and 500-580 MeV.

- The $\pi^0 J/\psi$ mode is susceptible to background from radiative lepton pair events where an extra "photon" is picked up to fake the π^0. We suppress these by requiring only barrel photons be used for the π^0, and that the π^0 center-of-mass decay angle satisfy $|\cos\alpha| < 0.75$, which requires the π^0 decays not to be too asymmetric.

- For the $\pi^0 J/\psi(\rightarrow e^+e^-)$ and $\eta(\rightarrow \gamma\gamma)J/\psi(\rightarrow e^+e^-)$ modes, background from Bhabha events with extra photons is partially suppressed with the cut $|\cos\theta_{e^+}| < 0.3$; this is effective because Bhabha events are dominated by the t-channel diagrams which have the final state e^+ preferentially scattered at small angles.

- For $X = \pi^0$ or $\eta(\rightarrow \gamma\gamma)$, background from radiative transitions (from $\psi(3770)$ or the $\psi(2S)$ tail) to χ_{c2} and χ_{c1} are suppressed by requiring the least energetic photon in the π^0 or η candidate to have energy exceeding 280 MeV or in the range 30-170 MeV.

IV. MONTE CARLO SAMPLES

To model the physics processes in a Monte Carlo procedure, we begin with a modified version (see below) of the `EvtGen` generator [26] including final state radiation [27], and a GEANT-based [28] detector simulation.

The process $e^+e^- \rightarrow \gamma\psi(2S)$ requires special care. We begin with a decay model which generates a final state with a photon and a vector meson with the correct angular distribution [29], inserting full initial state radiation effects according to the formulas below; specifically, the Breit-Wigner is generated out to $\sim \pm 285\Gamma$.

If E_γ denotes the photon energy, s the e^+e^- center-of-mass-energy squared, and M_{2S} the $\psi(2S)$ mass central value, then a scaled photon energy variable can be defined as $x \equiv 2E_\gamma/\sqrt{s}$, and $s' \equiv s(1-x)$ defined as the event-by-event mass-squared of the (broadly fluctuating) $\psi(2S)$. Then the differential cross section [30] for $e^+e^- \rightarrow \gamma\psi(2S) \rightarrow \gamma\ XJ/\psi$ as a function of s and x is

$$\frac{d\sigma}{dx}(s,x) = W(s,x) \times \sigma_{BW}(s') \times F(s') \times \mathcal{B}(\psi(2S) \rightarrow XJ/\psi) \tag{1}$$

where $W(s,x)$ represents the probability to emit a photon of scaled energy x from the initial state e^+e^-, $\sigma_{BW}(s)$ is the usual relativistic Breit-Wigner formula, and $F(s')$ is the appropriate phase space factor [31] for the given final state. The three functions W, σ_{BW}, and F can be written as

$$W(s, x > x_0) \equiv \frac{2\alpha}{\pi x}\left(\ln\frac{s}{m_e^2} - 1\right)\left(1 - x + \frac{x^2}{2}\right), \tag{2}$$

in which x_0 is a scaled photon energy cutoff to prevent the divergence of W, m_e is the electron mass and α is the fine structure constant;

$$\sigma_{BW}(s) \equiv \frac{12\pi\Gamma_{ee}\Gamma}{(s-M_{2S}^2)^2+M_{2S}^2\Gamma^2} \tag{3}$$

is a relativistic Breit-Wigner in which Γ (281 ± 17 keV [25]) and Γ_{ee} (2.12 ± 0.12 keV [25]) are, respectively, the full and di-electron partial widths of the $\psi(2S)$ and $M_{2S} \equiv$ 3686.093 MeV [25]; and the phase space factor is

$$F(s') \equiv \left(\frac{p_X}{p_0}\right)^{2L+1}, \tag{4}$$

in which p_X represents the average momentum of X in the $\psi(2S)$ center of mass frame, p_0 is the value of p_X at $\sqrt{s'} = M_{2S}$, and L is the relative orbital angular momentum between X and J/ψ.

The divergence in $W(s,x)$ as $x \to 0$ is handled in the way most MC event generators do: the above formulas are used for a photon energy above some cutoff (chosen here as $E_\gamma^{\rm cutoff}$=2 MeV), and then also generate events *without* a photon to represent all events with photons softer than the cutoff. The normalization for events below the cutoff, $W(s, x < x_0)$, includes terms accounting for soft and virtual photon emission as well as dileptonic and hadronic vacuum polarization, and can be calculated analytically [30]. For $s = s_0 = (3773 \text{ MeV})^2$ and $x_0 = 2E_\gamma^{\rm cutoff}/\sqrt{s_0}$, we find $\int W(s_0, x < x_0)\, dx = 0.67$, which has been checked empirically against a similar computation in the Babayaga [22] $\mu^+\mu^-$ event generator. The soft piece amounts to $\sim 1\%$ of the total radiative return cross section, depending on the phase space for each exclusive final state.

The radiative photon cutoff energy should be small enough that lumping together all events with energies below that value are experimentally indistinguishable from events just above the cutoff; if they were, then a discontinuity could appear in some distributions. On the other hand, the cutoff must be large enough so that the statistics near the photon cutoff energy in the radiative return MC do not limit the analysis. The choice of 2 MeV satisfies both criteria.

The center-of-mass energy determines the energy of the peak of the radiative return cross section as shown in Fig. 2, and the spread of such energies will affect the width of the radiative return photon energy peak. The MC sample used for this analysis has a mean and spread of $\sqrt{s}$ very close to that of the data (within 0.05 MeV and 0.02 MeV, respectively).

V. ANALYSIS METHOD

If both sides of the radiative return cross section in Eq. (1) are integrated, the total cross section for $e^+e^- \to \gamma\psi(2S) \to \gamma X J/\psi$ is obtained as

$$\sigma(s) = \frac{N}{\epsilon \times \mathcal{L}} = \Gamma_{ee} \times \mathcal{B}(\psi(2S) \to XJ/\psi) \times \int W(s,x)\frac{\sigma_{BW}(s')}{\Gamma_{ee}}F(s')dx \tag{5}$$

in which σ is the total cross section, which can be measured (N is the number of events seen, ϵ is the detection efficiency, and $\mathcal{L}$ is the integrated luminosity), and other symbols have been defined previously. The integral on the right in Eq. (5) has no unknowns and can be performed numerically, allowing determination of the product $\Gamma_{ee} \times \mathcal{B}(\psi(2S) \to XJ/\psi)$.

A. Extracting the background and signal yields

For the exclusive XJ/ψ modes we select events as described and then fit a distribution in a missing momentum variable we call k, which can be interpreted as the radiative photon energy In this variable, events that peak at 87 MeV are due to radiative returns and events that peak at zero represent a possible signal for direct $\psi(3770)$ decay (to the extent that the number exceeds that predicted by the tail of the $\psi(2S)$). We use the usual kinematic formulas in such a way as to deweight the effect of the leptons (the higher momentum, less well-measured, tracks) in the resolution. The expression for k can be obtained by writing out the two ways of computing the mass recoiling against the X "particle" (which could be $\pi\pi$), one using the properties of X only and the known center-of-mass momentum and energy, and the other from the measured J/ψ momentum and direction and the unknown momentum of a missing photon k:

$$(E_{cm} - E_X)^2 - (\mathbf{p_{cm}} - \mathbf{p_X})^2 = (k + \sqrt{p_J^2 + M_J^2})^2 - (\mathbf{p_J} + \mathbf{k})^2 \tag{6}$$

which, after a few lines of algebra, can be reduced to

$$k = \frac{E_{cm}^2 - M_J^2 + m_X^2 - 2E_{cm}\sqrt{p_X^2 + m_X^2}}{2\left(\sqrt{p_J^2 + M_J^2} - p_J \cos\phi\right)} \tag{7}$$

in which M_J=3.097 GeV is the J/ψ mass, $\mathbf{p_J}$ is the measured dilepton momentum, $\mathbf{p_X}$ is the measured X momentum, m_X is the mass of X (a fixed number for $X = \eta$ or $X = \pi^0$, or the measured mass for $X = \pi\pi$), ϕ is the measured angle between the J/ψ and the event missing momentum 3-vector, and the small ($\sim$2 mrad) crossing angle of the incoming $e^{\pm}$ beams has been neglected. For radiative returns to the $\psi(2S)$, $k \approx 87$ MeV, and this expression depends mostly on the measured properties of the system X, with corrections from the J/ψ momentum and direction amounting to as much as $\pm$5 MeV. The missing momentum k has about 20% better resolution on $\gamma\pi^+\pi^- J/\psi$ events than the $\pi^+\pi^-$ recoil mass alone.

The measured k distribution can be used for two purposes: determination of the yield of direct $\psi(3770) \to XJ/\psi$ from the peak at $k = 0$ MeV (in excess of the radiative return component), and the dielectron width of the $\psi(2S)$, as can be seen from Eq. (7).

B. Integrals of the Radiative Return Cross Section

The integration for $E_\gamma > 2$ MeV is accomplished by throwing pseudo-random points uniformly in a photon energy versus relative cross section rectangle and counting what fraction of them lies underneath the known differential cross section. Results for the numerical integrations are shown in Table I. We find that a statistical accuracy of $\sim$0.1% can be obtained by throwing points with photon energy from 2-160 MeV with $\sim 1 \times 10^9$ trials, which has efficiency of landing a point under the $d\sigma/dx$ curve of $\sim$0.24%. The table includes the effects of beam energy spread and of phase space for the particular final state as shown, and the soft photon term is shown and added to form the total radiative return cross section. These integrals are tabulated exclusive of (i.e. not including) the branching fraction of the $\psi(2S) \to XJ/\psi$ decay and dielectron width Γ_{ee} of the $\psi(2S)$, obtaining a value in units of cross section per energy unit. That is, to obtain the actual total cross section for the final

state XJ/ψ in question, one would have to multiply the value computed in this way by the product $\Gamma_{ee} \times \mathcal{B}(\psi(2S) \to XJ/\psi)$. The integral has only very weak dependence upon the full width Γ ($< 0.1\%$ for a change in Γ from the PDG [25] fit central value of 281 keV of one standard deviation, 17 keV); what sensitivity to Γ exists resides almost exclusively in the soft photon term, which has linear Γ dependence but very small overall weight. The table also shows that getting the mean beam energy right is moderately important, as changes of $\pm 1.5\%$ are induced by shifts of 1 MeV in E_{cm}, and that precise knowledge of the beam energy spread is not crucial.

The phase space [31] factors for π^0 and η are simple to calculate. The η momentum increases from $\sim$200 MeV/c to $\sim$356 MeV/c and the π^0 momentum from $\sim$527 MeV/c to $\sim$600 MeV/c. The phase space factors for $\eta J/\psi$ and $\pi^0 J\psi$ will scale with the cube of the J/ψ momentum since each has a P-wave orbital angular momentum state.

The phase space [31] factor for $\pi\pi$ is more complicated since the $\pi\pi$ mass varies over a range of $\sim$300 MeV. The *average* momentum of the $\pi\pi$ system increases by $\sim$11% (from $\sim$247 MeV/c to $\sim$275 MeV/c) from $\sqrt{s}$=3.686 GeV to 3.773 GeV. As the $\pi\pi$ and J/ψ are in a relative S-wave, and S-wave phase space for a fixed mass particle scales linearly with the its momentum, we expect only approximate $\sim$11% increase in the phase space factor over the full range of masses and momentum. For $\psi(2S)$ produced with masses in between 3.686 GeV and 3.773 GeV we use a phase space factor which scales linearly with the radiative photon energy. The functional form of phase space scaling between zero and 87 MeV photon energy is not crucial because the total phase space change is only 11% and the differential cross section is very small over most of this interval.

The phase space factors have a $\sim$0.1% effect on the "hard" photon ($E_\gamma > 2$ MeV) integrals for $\pi\pi$ and π^0, and increase the η integrals by just over 1%. Where the factors enter more dramatically is in $\sigma(x < x_0)$, where the factor is $\sim$5.64 for η, $\sim$1.11 for $\pi\pi$, and $\sim$1.48 for π^0.

VI. RESULTS

The distributions of missing momentum for the exclusive modes are fit to three components with floating normalization: a radiative return to $\psi(2S)$ contribution, which extends into the signal region but which has normalization set by the population near the radiative return peak at $\sim$87 MeV; a direct decay $\psi(3770) \to XJ/\psi$ signal contribution, which absorbs any remaining events near zero missing momentum that the $\psi(2S)$ radiative tail does not account for; and a background component linear in missing momentum to allow for the remaining feature of the data distributions. For each mode, the histogram representing the $\psi(2S)$ tail comes from merging those from two MC sources, one with radiative photons and one without. The cross sections in Table I dictate the fixed relative weight of the two contributions: $\sim$200:1 for $\pi\pi$, $\sim$40:1 for η, and $\sim$150:1 for π^0.

The distributions and fits are shown in Figs. 3-5. The fit results and quantities derived from them are shown in Table II. The efficiencies shown include the correction factors detailed in Ref. [24], the visible cross sections use the $\mathcal{B}(J/\psi \to \ell^+\ell^-) = (5.953 \pm 0.056 \pm 0.042)\%$ from Ref. [23], and the Γ_{ee} values use the $\mathcal{B}(\psi(2S) \to XJ/\psi)$ results shown from Ref. [24]. Statistical significances of the $\psi(3770)$ signals, obtained from the differences in log-likelihoods of the fits with and without a signal component included, are shown, indicating an unambiguous (13σ significance) $\pi^+\pi^- J/\psi$ signal, a strong (3.8σ significance) $\pi^0\pi^0 J/\psi$ signal, and a suggestive (2.2σ significance) $\eta J/\psi$ signal. In the absence of any

compelling evidence for significant non-$D\bar{D}$ decays of the $\psi(3770)$, the recent precision measurement [32], $\sigma(D\bar{D}) = 6.39 \pm 0.10^{+0.17}_{-0.08}$ nb, is used along with the integrated luminosity (281 ± 2.8 pb^{-1}) to estimate the number of $\psi(3770)$ decays in the final sample as $(1.80 \pm 0.03^{+0.06}_{-0.02}) \times 10^6$, where we have added an additional high-side relative uncertainty of 2% to account for possible non-$D\bar{D}$ $\psi(3770)$ decays. Systematic errors from the fits, the efficiencies, radiative return cross section integrals, intermediate branching fractions, and luminosity are included.

Table III summarizes the uncertainties relevant to the quantities being measured. The efficiency uncertainties are larger than those appearing in the $\psi(2S) \to XJ/\psi$ analysis [24] because here the leptons are not restricted to the barrel, the cut is harder on the $\pi^+\pi^-$ invariant mass, the $\pi^0 \to \gamma\gamma$ mass cuts are somewhat tighter, and, for the radiative return events, we account for possible mismodeling of the $\psi(2S)$ boost direction. The systematic error on the fitted event yields accounts for varying the range in missing momentum of the fit, the shape of the background function, and the effect of the data having slightly worse resolution than the simulation. Statistical errors dominate for the $\psi(3770)$ results and systematic errors dominate for the $\psi(2S)$ results.

The $\pi^0 J/\psi$ radiative return yield shown has been reduced by 10 events from the fit value to account for background expected from $\psi(2S)$ two photon cascade decays to J/ψ through χ_{cJ}. MC studies also show that substantial background is expected from radiative Bhabha and radiative muon pair events, but the precise level of this background is difficult to estimate since it amounts to such a small fraction of the total Bhabha or muon pair cross sections. For this reason, the radiative return values for $\pi^0 J/\psi$ are all treated as upper limits. The statistical error on the direct $\psi(3770)$ decay yield (essentially zero) yields the upper limits at 90% C.L. shown.

We compute a value for Γ_{ee} by combining results from $\pi^+\pi^- J/\psi$, $\pi^0\pi^0 J/\psi$, and $\eta J/\psi$, weighting by the uncorrelated statistical and systematic errors, and adding back the correlated uncertainties after weighting, resulting in $\Gamma_{ee} = 2145 \pm 85$ eV. The relative 4.0% uncertainty includes both statistical and systematic errors, but is dominated by the common 3% systematic normalization uncertainty in all CLEO $\psi(2S)$ branching fraction measurements.

The branching fractions allow us to set a 90% C.L. upper limit for $\mathcal{B}(\psi(3770) \to XJ/\psi)$, $X = \pi\pi,\ \eta,\ \pi^0$ of 0.66%, or a corresponding cross section upper limit of 42 pb. This will become a useful after an inclusive $\psi(3770)$ cross section is measured with precision.

Fig. 6 shows the folded ℓ^+ polar angle distribution of $\pi^+\pi^- J/\psi$, $J/\psi \to \ell^+\ell^-$ events with $m(\pi^+\pi^-\text{recoil}) = 3.085 - 3.105$ GeV, background subtracted with the scaled 3.11-3.15 GeV sideband. The MC assumes relative S-wave between the $\pi\pi$ and the J/ψ; the confidence level of the data-MC consistency is $\sim$10%.

Fig. 7 shows the dipion mass of $\pi^+\pi^- J/\psi$ events with $m(\pi^+\pi^-\text{recoil}) = 3.085{-}3.105$ GeV, background subtracted with the scaled 3.11-3.15 GeV sideband. In some models [2, 4–6] this distribution is much softer if a strong D-wave component between $\pi\pi$ and J/ψ is present; however, the data and pure S-wave [26] Monte Carlo distributions agree moderately well here, but showing slightly *more* high-mass peaking in the data than the MC prediction.

VII. CONCLUSIONS

We observe a statistically unambiguous signal for $\psi(3770) \to \pi^+\pi^- J/\psi$ and strong evidence for $\psi(3770) \to \pi^0\pi^0 J/\psi$. The branching fraction for $\psi(3770) \to \pi^+\pi^- J/\psi$ is about half of that reported by BES [11], but is consistent with it and more precise. While the

widths for $\psi(3770) \to \pi\pi J/\psi$ are in the broad range predicted by the QCD multipole expansion models [2, 4–6], the $\pi\pi$ mass distribution appears to be much harder than predicted for the large ($> 50\%$) D-wave proportion these models favor. The observed width is small enough to add yet another argument against a conventional charmonium interpretation of $X(3872)$.

We observe only a hint of $\psi(3770) \to \eta J\psi$ production but consistent with the expected level, which is more than five times higher relative to $\pi^+\pi^- J/\psi$ than at the $\psi(2S)$ due to the phase space enhancement. Sensitivity to $\psi(3770) \to \pi^0 J\psi$ with the current dataset is low, with only a very loose limit set on its level. Both these values can be used to address the question of $c\bar{c}$ purity [18] of the $\psi(2S)$ and $\psi(3770)$: the 90% C.L. upper limits are $\mathcal{B}(\psi(3770) \to \eta J/\psi) < 0.14\%$, $\mathcal{B}(\psi(3770) \to \pi^0 J/\psi) < 0.026\%$, and the η to π^0 ratio is > 2.6. These provide initial constraints, but they are not stringent enough to firmly test the predictions. Substantially more data would be required to do so.

Our Γ_{ee} measurement is unique for several reasons: it does not come from a resonance scan, it depends on an assumed value of the full width Γ only very weakly, and it uses only CLEO measurements for the important intermediate branching fractions ($\mathcal{B}(\psi(2S) \to XJ/\psi)$ and $\mathcal{B}(J/\psi \to \ell^+\ell^-)$). It is consistent with but more precise than the PDG fit value (2.12 ± 0.12 keV) or any of the results obtained from scanning the peak, the most precise being the BES [33] result (2.44 ± 0.21 keV). It is also significantly more precise than can be obtained through measurements of $\mathcal{B}(\psi(2S) \to e^+e^-)$ [34, 35], partly due to the experimental precisions in these measurements, but also because the current relative uncertaintly on the full width Γ is $\sim$6%. Similarly, we use this measurement of Γ_{ee} to obtain $\mathcal{B}(\psi(2S) \to e^+e^-) = \Gamma_{ee}/\Gamma = (7.63 \pm 0.31 \pm 0.46) \times 10^{-3}$, in which the errors represent the uncertainties in Γ_{ee} and Γ, respectively. This value is limited by the full width Γ uncertainty, but it still compares well to and agrees with the more precise E835 [35] result (renormalized to the CLEO $\psi(2S) \to XJ/\psi$ and $J/\psi \to \ell^+\ell^-$ branching fractions), $(7.30 \pm 0.39) \times 10^{-3}$.

All results described here are preliminary.

Acknowledgments

We gratefully acknowledge the effort of the CESR staff in providing us with excellent luminosity and running conditions. This work was supported by the National Science Foundation and the U.S. Department of Energy.

[1] H.J. Lipkin, Phys. Lett. **B179**, 278 (1986).
[2] T.M. Yan, Phys. Rev. D **22**, 1652 (1980).
[3] K. Lane, Harvard Report No. HUTP-86/A045 (1986) (unpublished).
[4] Y.P. Kuang, Phys. Rev. D **65**, 094024 (2002).
[5] Y.P. Kuang and T.M. Yan, Phys. Rev. D **41**, 155 (1990).
[6] Y.P. Kuang and T.M. Yan, Phys. Rev. D **24**, 2874 (1981).
[7] J.L. Rosner, Phys. Rev. D **64**, 094002 (2001).
[8] CLEO Collaboration, G. Adams *et al.*, Cornell LEPP Report CLEO-CONF 05-02 (LP2005-439) (2005).

[9] CLEO Collaboration, G.S. Huang *et al.*, Cornell LEPP Report CLNS-05/1921 (LP2005-443) (2005).
[10] CLEO Collaboration, P. Rubin *et al.*, Cornell LEPP Report CLEO-CONF 05-11 (2005).
[11] BES Collaboration, J.Z. Bai *et al.*, Phys. Lett. **B605**, 63 (2005).
[12] T. Barnes and S. Godfrey, Phys. Rev. D **69**, 054008 (2004).
[13] E.J. Eichten, K. Lane, and C. Quigg, Phys. Rev. D **69**, 094019 (2004).
[14] Belle Collaboration, S.K. Choi *et al.*, Phys. Rev. Lett. **91**, 262001 (2003); CDF-II Collaboration, D. Acosta *et al.*, Phys. Rev. Lett. **93**, 072001 (2004); D0 Collaboration, V.M. Abazov *et al.*, Phys. Rev. Lett. **93**, 162002 (2004); BaBar Collaboration, B. Aubert *et al.*, Phys. Rev. D **71**, 071103 (2005).
[15] Belle Collaboration, K. Abe *et al.*, hep-ex/0505037 (LP2005-175) (2005).
[16] Belle Collaboration, K. Abe *et al.*, hep-ex/0505038 (LP2005-176) (2005).
[17] S.L. Olsen, Int. J. Mod. Phys **20**, 240 (2005).
[18] M.B. Voloshin, Phys. Rev. D **71**, 114003 (2005).
[19] CLEO-c/CESR-c Taskforces & CLEO-c Collaboration, Cornell LEPP preprint CLNS 01/1742 (2001).
[20] CLEO Collaboration, Y. Kubota *et al.*, Nucl. Instrum. Methods Phys. Res., Sect. A **320**, 66 (1992); D. Peterson *et al.*, Nucl. Instrum. Methods Phys. Res., Sect. A **478**, 142 (2002); M. Artuso *et al.*, Nucl. Instrum. Methods Phys. Res., Sect. A **502**, 91 (2003).
[21] CLEO Collaboration, G. Crawford *et al.*, Nucl. Instrum. Methods Phys. Res., Sect. A **345**, 429 (1992).
[22] C.M. Carloni Calame *et al.* in *Proceedings of the Workshop on Hadronic Cross-Section at Low-Energy (SIGHAD03), 8-10 October 2003, Pisa, Italy,* edited by M. Incagli and G. Graziano (Elsevier, Amsterdam, 2004), p. 258.
[23] CLEO Collaboration, Z. Li *et al.*, Phys. Rev. D **71**, 111103 (2005).
[24] CLEO Collaboration, N.E. Adam *et al.*, Phys. Rev. Lett. **94**, 232002 (2005).
[25] S. Eidelman *et al.*, Phys. Lett. **B592**, 1 (2004).
[26] D.J. Lange, Nucl. Instrum. Methods Phys. Res., Sect. A **462**, 152 (2001).
[27] E. Barberio and Z. Was, Comput. Phys. Commun. **79**, 291 (1994).
[28] R. Brun *et al.*, GEANT 3.21, CERN Program Library Long Writeup W5013 (1993), unpublished.
[29] M. Benayoun *et al.*, Mod. Phys. Lett. **A14**, 2605 (1999).
[30] J. Schwinger, Phys. Rev **76**, 760 (1949); G. Bonneau and F. Martin, Nucl. Phys. **B27**, 381 (1971); E.A. Kuraev and V.S. Fadin, Sov. J. Nucl. Phys. **41**, 466 (1985); J.P. Alexander *et al.*, Nucl. Phys. **B320**, 45 (1989).
[31] J.D. Jackson, Nuovo Cimento **34**, 1644 (1964); E852 Collaboration, S.U. Chung, *et al.*, Phys. Rev. D **60**, 092001 (1999).
[32] CLEO Collaboration, Q. He *et al.*, hep-ex/0504003 (2005) (submitted to Phys. Rev. Lett.).
[33] BES Collaboration, J.Z. Bai *et al.*, Phys. Lett. **B550**, 24 (2002).
[34] BABAR Collaboration, B. Aubert *et al.*, Phys. Rev. D **69**, 011103R (2004).
[35] E835 Collaboration, M. Andreotti *et al.*, Phys. Rev. D **71**, 032006 (2005).

TABLE I: Integrals of the radiative return cross section as a function of the center of mass energy E_{cm}, its spread ΔE_{cm}, and phase space factor F (unity, $\pi\pi$, η, and π^0). The cross sections σ are quoted without including the factor $\mathcal{B}(\psi(2S) \to XJ/\psi) \times \Gamma_{ee}$ and are in units of cross section per unit energy. The results quoted are for E_γ=2-160 MeV (and are insensitive to the exact value of the upper limit), more than 1 billion trials and therefore better than 0.1% statistical accuracy for each point. The values varied from one line to the next are underlined.

E_{cm} (GeV)	ΔE_{cm} (GeV)	F	$\sigma(E_\gamma >2$ MeV) (pb/keV)	$\sigma(E_\gamma <2$ MeV) (pb/keV)	σ_{sum} (pb/keV)
3.7723	0.0023	1	1456.4	6.7	1463.1
3.7733	0.0023	1	1437.7	6.5	1444.2
3.7743	0.0023	1	1420.5	6.4	1426.9
3.7733	0.0021	1	1437.6	6.5	1444.1
3.7733	0.0025	1	1438.0	6.5	1444.5
3.7733	0.0023	$\pi\pi$	1441.4	7.2	1448.6
3.7733	0.0023	η	1454.2	36.7	1490.9
3.7733	0.0023	π^0	1437.9	9.6	1447.5

TABLE II: Results for radiative return process $e^+e^- \to \gamma\psi(2S)$, $\psi(2S) \to XJ/\psi$ and direct decay $\psi(3770) \to XJ/\psi$. For each appears the fit yield N, efficiency ϵ, and cross section σ (obtained using $\mathcal{B}(J/\psi \to \ell^+\ell^-)$ from ref. [23]). In addition, for the radiative return process, the $\mathcal{B}(\psi(2S) \to XJ/\psi)\times\Gamma_{ee}$ values inferred from the cross section and the integrals in Table I appear, and, using the exclusive branching fractions $\mathcal{B}(\psi(2S) \to XJ/\psi)$ from ref. [24], the resulting Γ_{ee}. The bottom five rows include the significance in standard deviations of the $\psi(3770) \to XJ/\psi$ signals obtained from the likelihood differences of fits with and without a signal component, and the $\psi(3770)$ branching fraction using the number of produced $\psi(3770)$ events as $(1.80 \pm 0.03^{+0.06}_{-0.02}) \times 10^6$ [32] with an extra 2% high side uncertainty added to account for potential non-$D\bar{D}$ decays. Errors shown are statistical and systematic, respectively.

Mode XJ/ψ	$\pi^+\pi^-\ell^+\ell^-$	$\pi^0\pi^0\ell^+\ell^-$	$\eta\ell^+\ell^-$	$\pi^0\ell^+\ell^-$
$N(\gamma\psi(2S))$	$16923 \pm 157 \pm 169$	$3592 \pm 85 \pm 72$	$275 \pm 26 \pm 8$	< 37
ϵ (%)	$48.03 \pm 0.07 \pm 0.72$	$21.66 \pm 0.06 \pm 0.45$	$7.77 \pm 0.17 \pm 0.14$	$11.3 \pm 0.1 \pm 0.4$
σ (pb)	$1053 \pm 14 \pm 23$	$496 \pm 13 \pm 16$	$105.7 \pm 10.3 \pm 5.0$	< 9.8
$\mathcal{B} \times \Gamma_{ee}$ (eV)	$727 \pm 10 \pm 16$	$342 \pm 9 \pm 11$	$70.9 \pm 6.9 \pm 3.4$	< 6.8
$\mathcal{B}$ (%) [24]	$33.54 \pm 0.14 \pm 1.10$	$16.52 \pm 0.14 \pm 0.58$	$3.25 \pm 0.06 \pm 0.11$	$0.13 \pm 0.01 \pm 0.01$
Γ_{ee} (eV)	$2168 \pm 30 \pm 85$	$2072 \pm 56 \pm 98$	$2181 \pm 216 \pm 128$	< 5220
$N(\psi(3770))$	$217 \pm 25 \pm 2$	$42.2 \pm 16.1 \pm 0.8$	$17.1 \pm 11.4 \pm 0.5$	< 7.6@90% C.L.
Signif.	13σ	3.8σ	2.2σ	0σ
ϵ (%)	$53.70 \pm 0.19 \pm 0.81$	$22.67 \pm 0.20 \pm 0.48$	$12.01 \pm 0.19 \pm 0.22$	$13.67 \pm 0.15 \pm 0.44$
σ (pb)	$12.1 \pm 1.4 \pm 0.3$	$5.6 \pm 2.1 \pm 0.2$	$4.2 \pm 2.8 \pm 0.2$	< 1.7@90% C.L.
$\mathcal{B}$ (10^{-5})	$189 \pm 22^{+7}_{-4}$	$87 \pm 33 \pm^{+4}_{-3}$	$67 \pm 44^{+4}_{-3}$	< 26@90% C.L.

TABLE III: Relative uncertainties in percent for the branching fractions, cross sections, $\mathcal{B} \times \Gamma_{ee}$, and Γ_{ee} measurements, as applicable. The numbers in parentheses in the first row apply to the direct decay $\psi(3770) \to XJ/\psi$ cross section determinations; all other rows' entries apply to both radiative return and direct decay measurements. The rows labelled with a superscripted asterisk* signify those which have the same, completely correlated uncertainty for all modes.

Source	$\pi^+\pi^-$	$\pi^0\pi^0$	η	π^0
Event yield (stat)	1.3 (9.7)	1.8 (29)	6.5(46)	19 (-)
Event yield (sys)	1.0	2.0	3.0	1.0
Efficiency	1.5	2.1	1.8	3.2
Backgrounds	0.1	0.1	3.0	50
Radiative Corrections*	1.0	1.0	1.0	1.0
Luminosity*	1.0	1.0	1.0	1.0
$\mathcal{B}(J/\psi \to \ell^+\ell^-)$ stat*	0.94	0.94	0.94	0.94
$\mathcal{B}(J/\psi \to \ell^+\ell^-)$ sys*	0.71	0.71	0.71	0.71
$\mathcal{B}(\psi(2S) \to XJ/\psi)$ stat	0.42	0.85	1.85	7.7
$\mathcal{B}(\psi(2S) \to XJ/\psi)$ sys	1.33	1.82	1.57	7.1
$\mathcal{B}(\psi(2S) \to XJ/\psi)$ sys*	3.0	3.0	3.0	3.0

FIG. 1: Distribution of the radiative photon energy for $e^+e^- \to \gamma\psi(2S)$ (see text) with the photon energy cutoff set at 2 MeV (as in Eq. (1)).

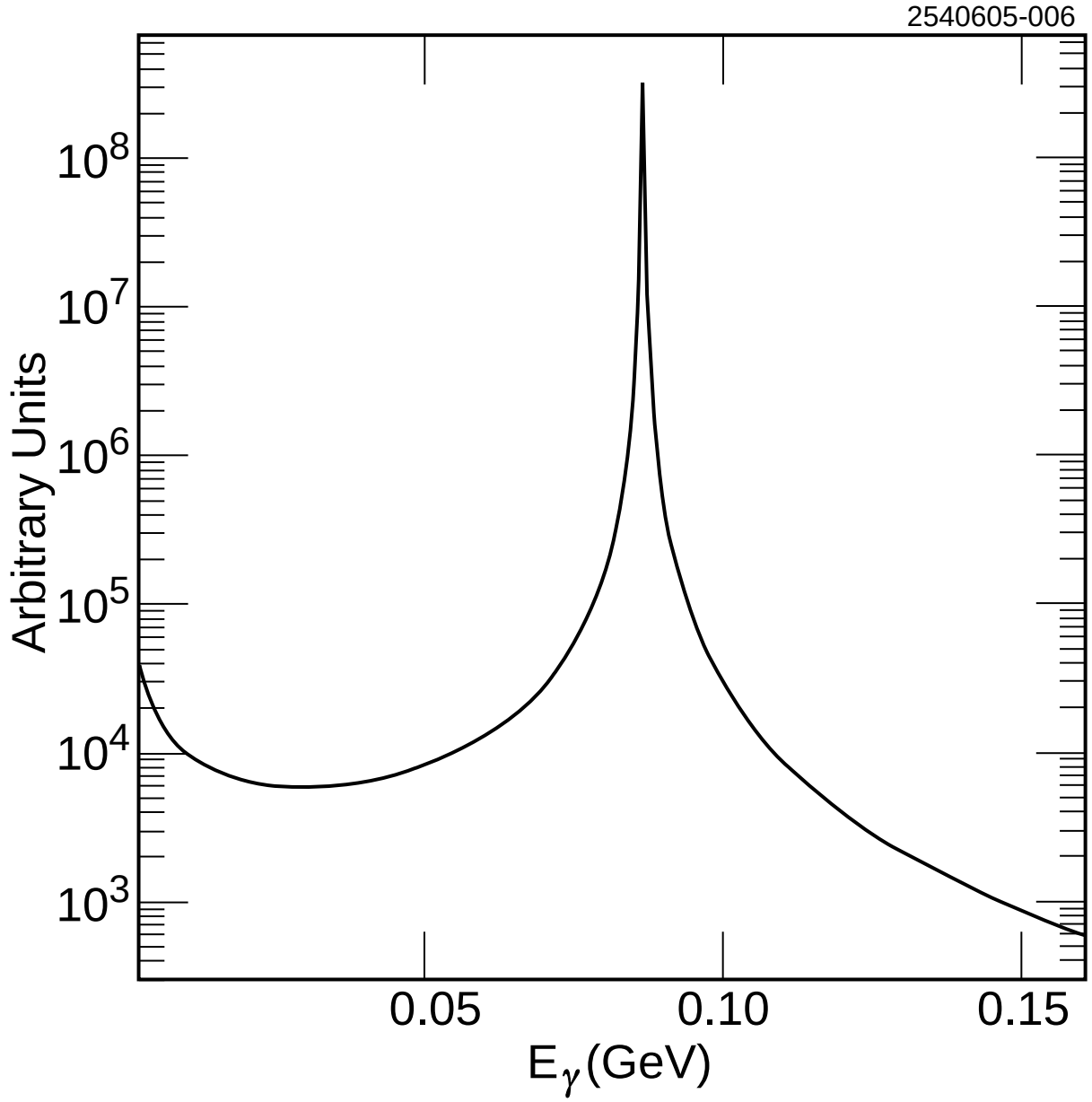

FIG. 2: Distribution of the radiative photon energy for $e^+e^- \to \gamma\psi(2S)$ for the three choices of center-of-mass energy: mid-range ($\sqrt{s}$ = 3.77316 GeV, solid black line), high-end ($\sqrt{s}$ = 3.7741 GeV, dotted red line), and low-end ($\sqrt{s}$ = 3.7708 GeV, dashed green).

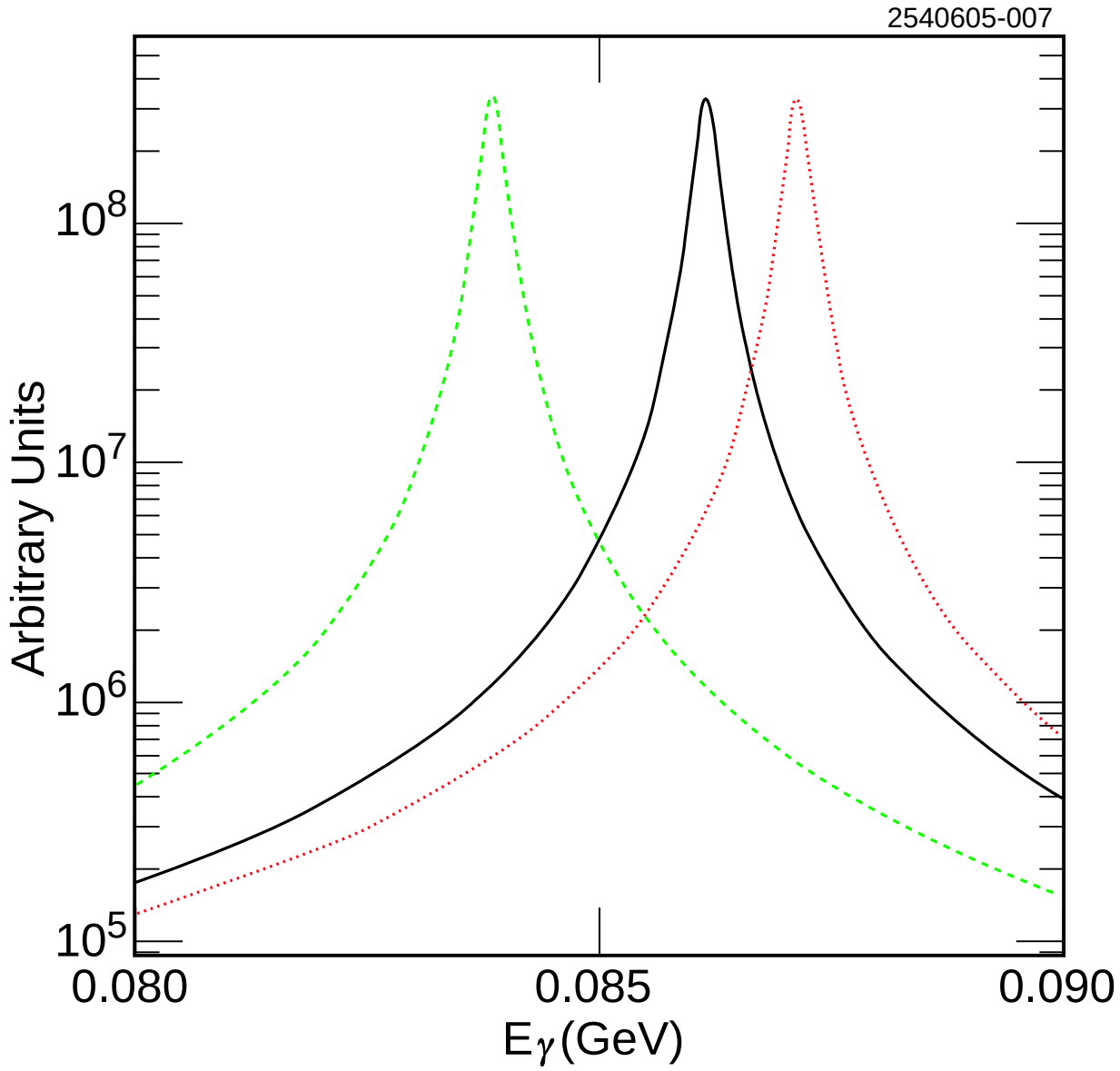

FIG. 3: Fit of the event missing momentum distribution for the final state $\pi^+\pi^- J/\psi$, $J/\psi \to \ell^+\ell^-$, showing the data (open circles), total fit (black dot-dash histogram), direct $\psi(3770)$ decay peak (solid red histogram), radiative return to the $\psi(2S)$ (blue dotted histogram), and the background term (dashed green histogram), on a logarithmic vertical scale (top), and on linear vertical scales zoomed in on the direct decay peak (bottom left) and radiative return peak (bottom right).

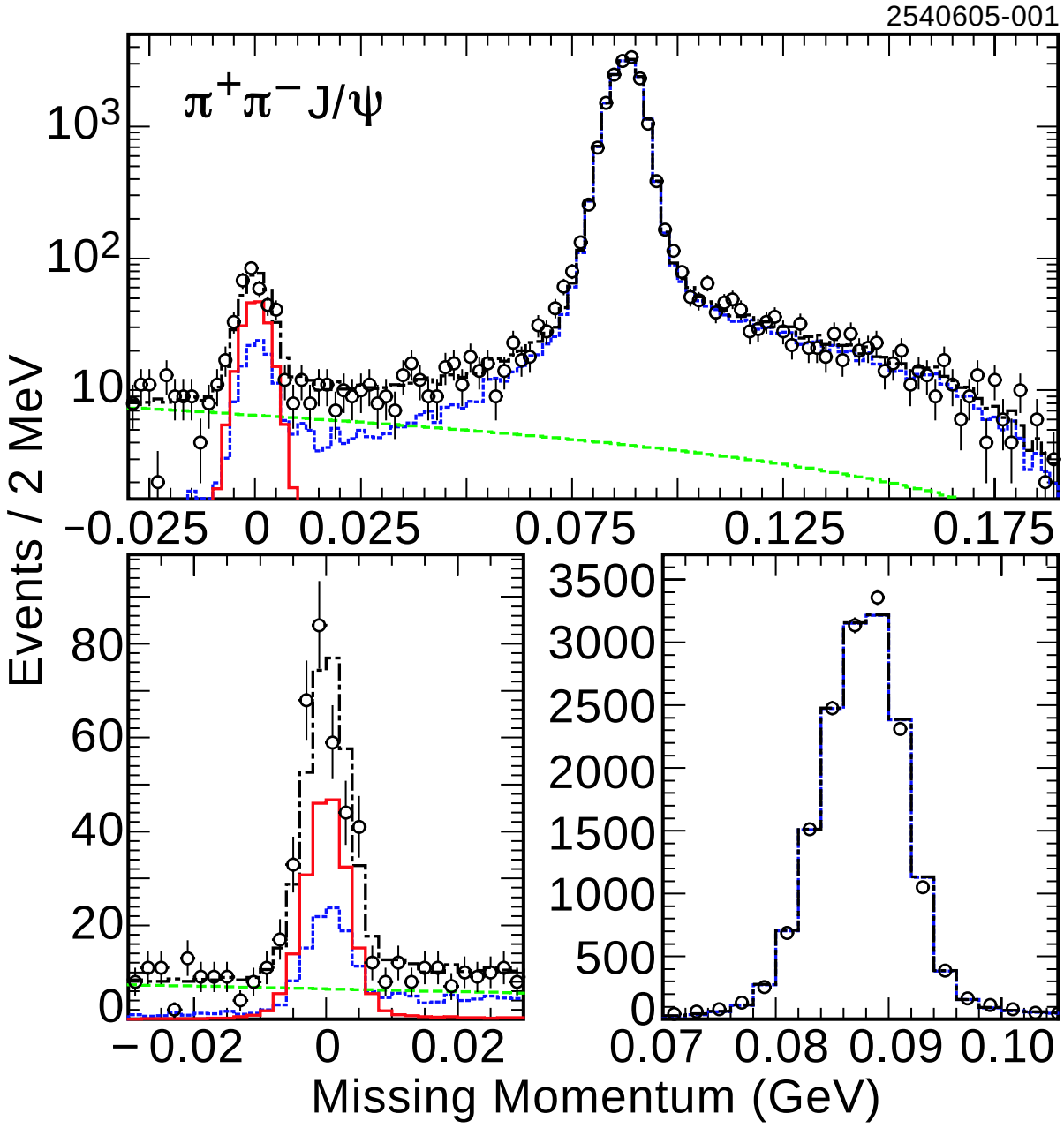

FIG. 4: Fit of the event missing momentum distribution for the final state $\pi^0\pi^0 J/\psi$, $J/\psi \to \ell^+\ell^-$, showing the data (open circles), total fit (black dot-dash histogram), direct $\psi(3770)$ decay peak (solid red histogram), radiative return to the $\psi(2S)$ (blue dotted histogram), and the background term (dashed green histogram), on a logarithmic vertical scale (top), and on linear vertical scales zoomed in on the direct decay peak (bottom left) and radiative return peak (bottom right).

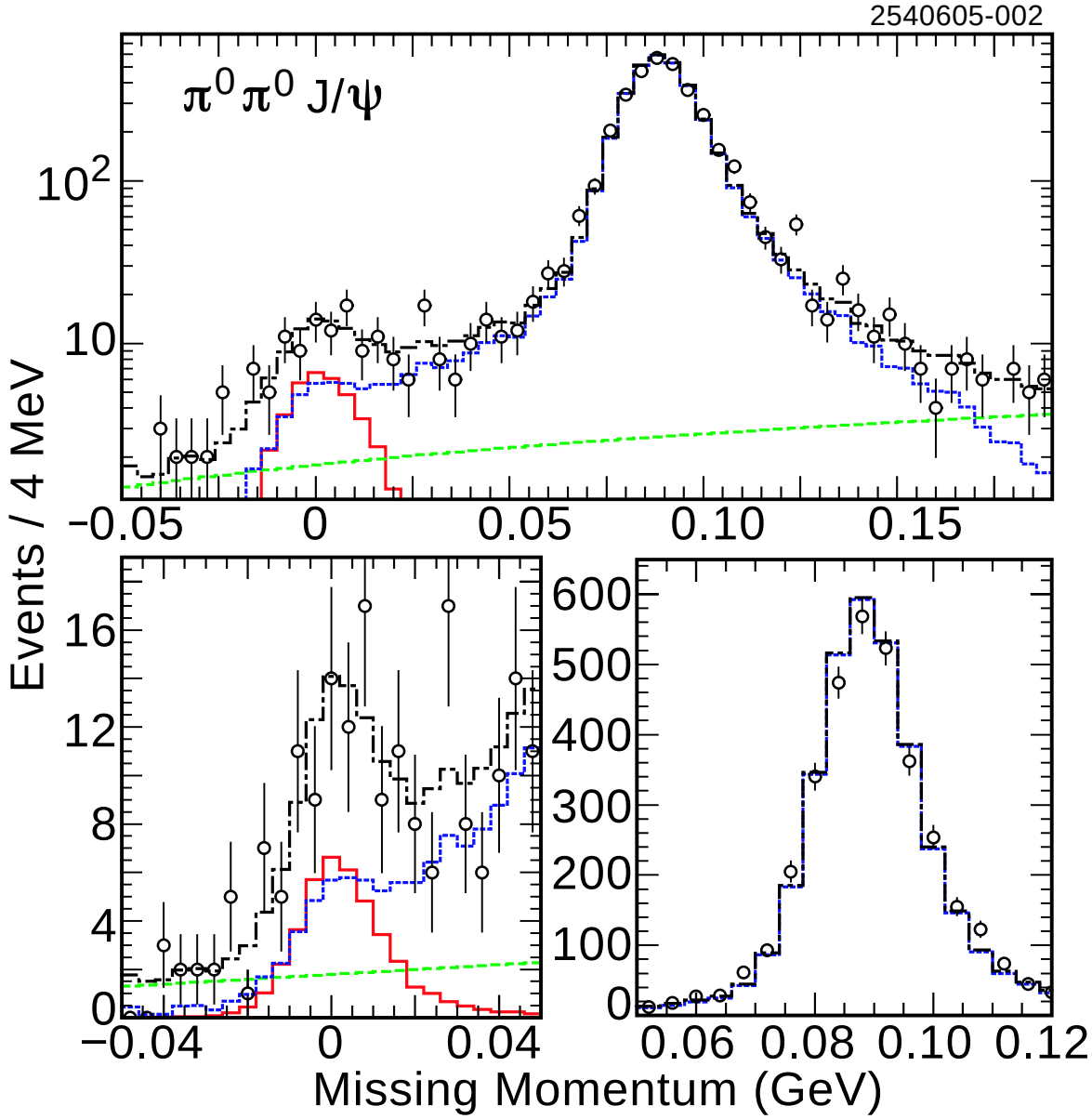

FIG. 5: Fit of the event missing momentum distribution for the final state $\eta J/\psi$ (top) and $\pi^0 J/\psi$ (bottom), $J/\psi \to \ell^+\ell^-$, showing for each the data (open circles), total fit (black dot-dash histogram), direct $\psi(3770)$ decay peak (solid red histogram), radiative return to the $\psi(2S)$ (blue dotted histogram), and the background term (dashed green histogram).

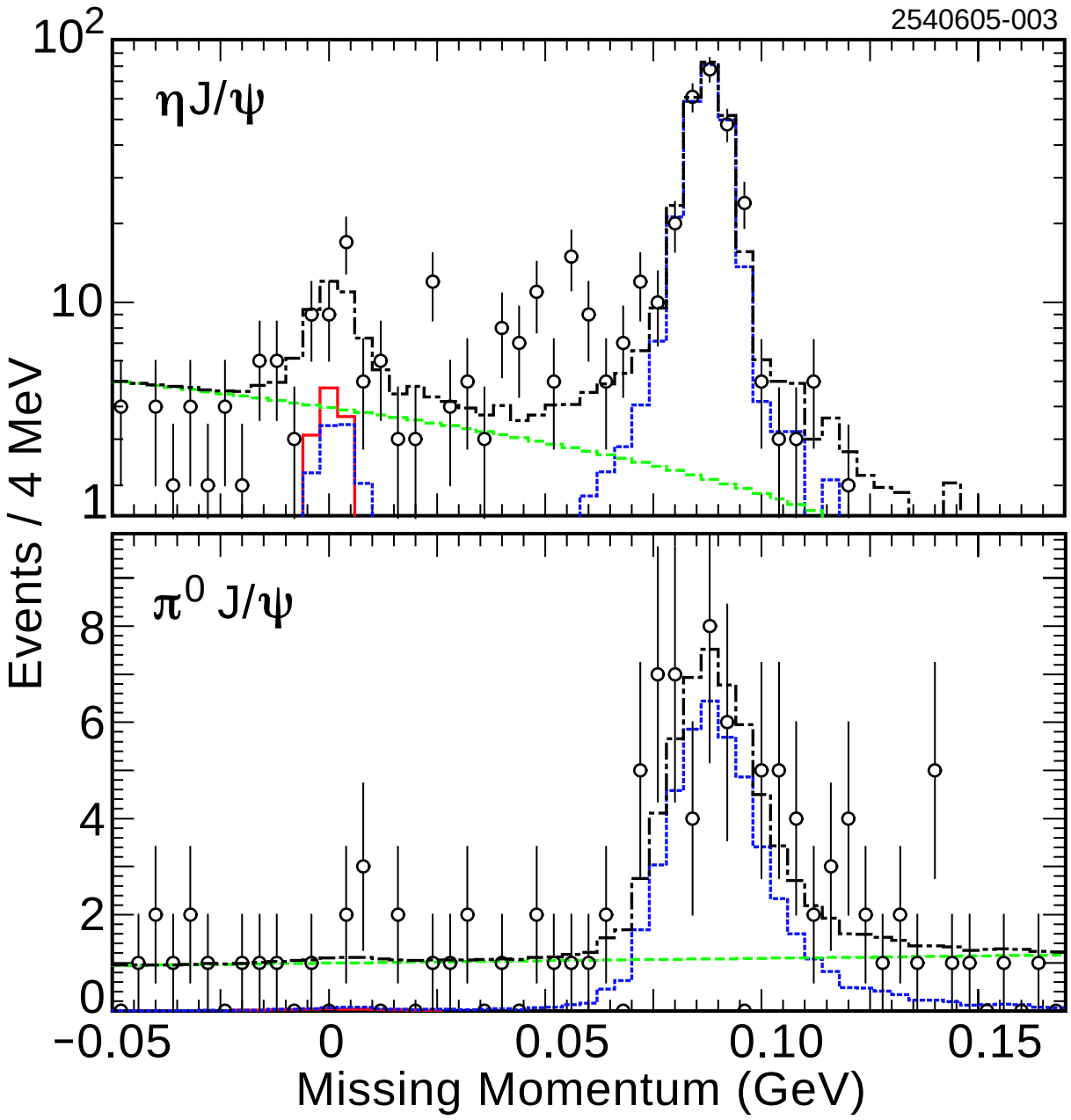

FIG. 6: Distribution on $\pi^+\pi^-\ell^+\ell^-$ events of the polar direction of the positively charged lepton from data (open circles) and MC (solid histogram).

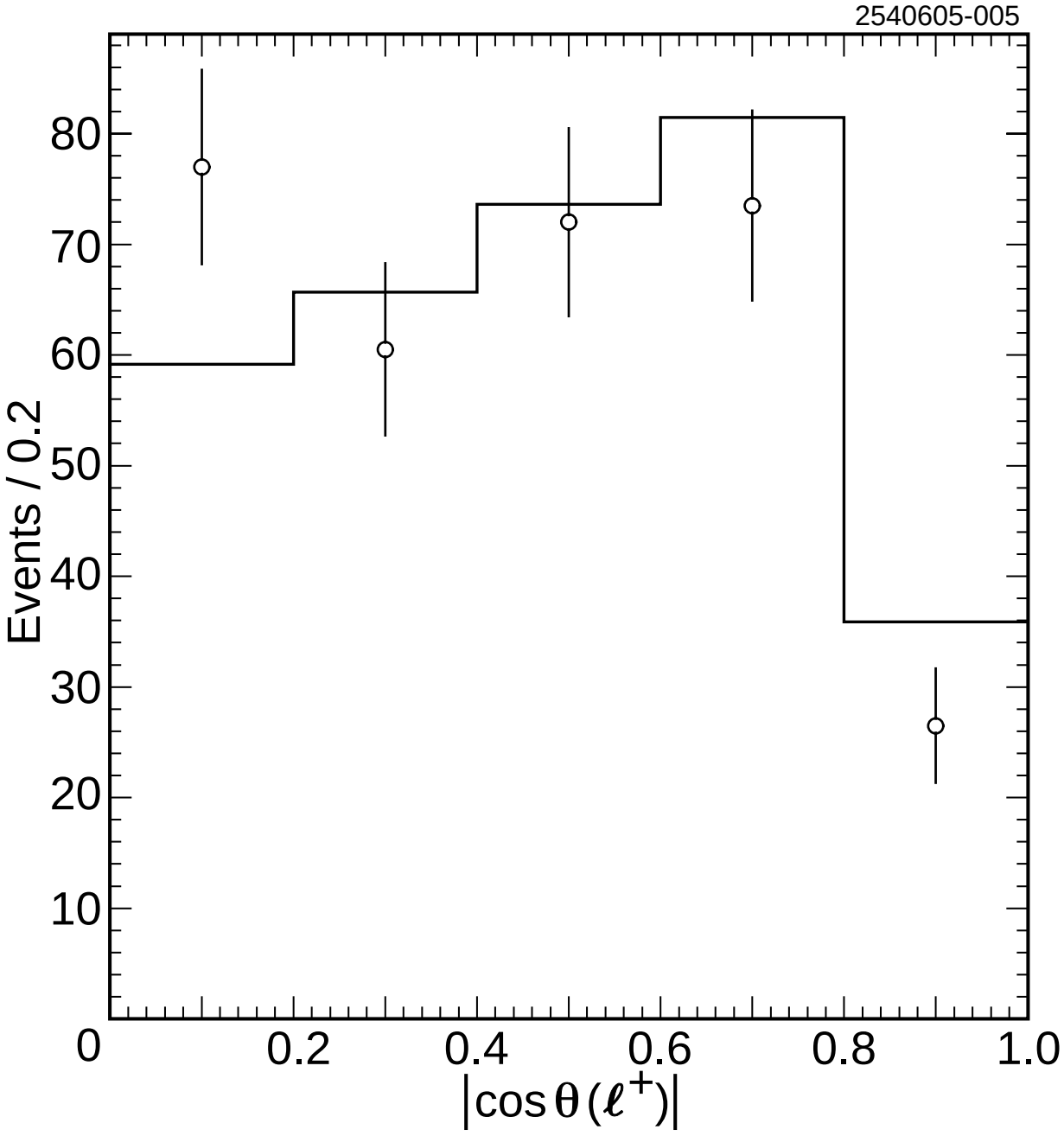

FIG. 7: Distribution on $\pi^+\pi^-\ell^+\ell^-$ events of the $\pi^+\pi^-$ mass from data (open circles) and MC (solid histogram).